Sodium Phosphaethynolate, Na(OCP), as a "P" Transfer Reagent for the Synthesis of N-Heterocyclic Carbene Supported P_3 and PAsP Radicals

Aaron M. Tondreau,[a] *Zoltán Benkő,*[a] *Jeffery Harmer,*[b] *Hansjörg Grützmacher*[a,c]*

[a] *Department of Chemistry and Applied Biosciences, ETH Zürich, CH-8093, Switzerland,* hgruetzmacher@ethz.ch
[b] *Centre for Advanced Imaging, University of Queensland, St Lucia, QLD 4072, Australia,* jeffrey.harmer@cai.uq.edu.au
[c] *Lehn Institute of Functional Materials (LIFM), Sun Yat-Sen University, 510275 Guangzhou, China.*

Supporting Information

Experimental Section

General Considerations. All air- and moisture-sensitive manipulations were carried out using standard vacuum line Schlenk techniques or in an MBraun inert atmosphere dry-box containing an atmosphere of purified argon. THF and n-hexane were distilled from sodium benzophenone ketyl before use. THF-d_8 and CD_2Cl_2 were purchased from Cambridge Isotope Laboratories and dried over 4 Å molecular sieves. The compounds: Na(OCP),[i] $P_7(TMS)_3$,[ii] and [^{Dipp}NHC-H][Cl][iii] were synthesized according to literature procedures.

^{1}H NMR spectra were recorded on Bruker 300 or 500 spectrometers operating at 300.130 and 500.260 MHz, respectively. ^{13}C NMR spectra were recorded on a Bruker 500 spectrometer operating at 125.790 MHz. ^{31}P NMR spectra were recorded on Bruker 300 or 500 spectrometers operating at 121.494 and 202.509 MHz, respectively. All ^{1}H and ^{13}C NMR chemical shifts are reported relative to $SiMe_4$ using the ^{1}H (residual) and ^{13}C chemical shifts of the solvent as a secondary standard. Infrared spectra were collected on a Perkin-Elmer-Spectrum 2000 FT-IR-Raman spectrometer. UV/vis spectra were recorded on UV/vis/NIR lambda-19-spectrometer in a cell with a 1 cm path length. Elemental analyses were performed at the Mikrolabor of ETH Zürich. Reliable elemental analysis data proved difficult to obtain due to the sensitivity of the samples. Alternative bulk methods of characterization are provided as evidence of the efficacy of the syntheses. Powder X-ray diffraction patterns of the samples were recorded with a STOE Stadi P diffractometer equipped with a germanium monochromator and $\mathrm{CuK}_{\alpha1}$ radiation (operated at 35 mA, 35 kV). Powder spectra were simulated using: WinXPow Version 3.0.1.13 (06-Dec-2010), STOE&Cie GmbH, 64295 Darmstadt, Germany.

X-ray diffraction studies

Single crystals suitable for X-ray diffraction were coated with polyisobutylene oil in a dry-box, transferred to a nylon loop and then transferred to the goniometer of a Bruker X8 APEX2 diffractometer equipped with a molybdenum X-ray tube (λ = 0.71073 Å) or to a Bruker D8 Venture equipped with both a molybdenum X-ray tube (λ = 0.71073 Å) and a copper X-ray tube (λ = 1.54178 Å). Preliminary data was collected to determine the crystal system. A hemisphere routine was used for data collection. The space group was identified and the data were processed using the Bruker SAINT+ program and corrected for absorption using SADABS. The structures were solved using direct methods (SHELXS) completed by Fourier synthesis and refined by full-matrix least-squares procedures.

Table S1: Crystal data and structure refinement details.[a]

Compound	**$^{\mathrm{Dipp}}$NHC=PH (4)**	**[($^{\mathrm{Dipp}}$NHC)$_2$(μ-P$_3$)]-[Cl] (7)**	**($^{\mathrm{Dipp}}$NHC)$_2$(μ-P$_3$) (9)**	**[($^{\mathrm{Dipp}}$NHC)$_2$(μ-PAsP)][Cl] (8)**
Formula	$C_{27}H_{37}N_2P$	$C_{58}H_{80}N_4OP_3$	$C_{54}H_{72}N_4P_3$	$C_{66}H_{96}AsClN_4O_3P_2$
M	420.56	977.66	870.07	1165.78
Cryst. Syst.	Monoclinic	Monoclinic	Triclinic	Monoclinic
Space Gr.	C2/c	P2(1)/c	P-1	C2/c
A [Å]	20.061(1)	17.0305(12)	11.9151(2)	24.9280(12)
B [Å]	6.986(1)	21.4738(9)	13.5428(2)	14.1030(7)
C [Å]	38.187(3)	16.7809(11)	15.8914(3)	17.8654(8)
α [deg]	90	90	85.680(1)	90
β [deg]	102.741(2)	115.996(3)	89.601(1)	92.468(2)
Γ [deg]	90	90	79.255(1)	90
U [Å]	5219.7(7)	5516.0(6)	2512.11(7)	6274.9(5)
Z	8	4	2	4
Total reflns.	8261	16829	11593	7769
Data Compl.	0.994	1.000	0.996	0.999
Theta(max)	31.000	30.510	27.54	28.28
R(reflns)	0.0461(6513)	0.0441(12024)	0.0465 (7850)	0.0414(6192)
wR$_2$ (reflns)	0.1543(8261)	0.1329(16821)	0.1180(11545)	0.1053(7764)
Compound	**($^{\mathrm{Dipp}}$NHC)$_2$(μ-PAsP) (10)**	**[($^{\mathrm{Dipp}}$NHC)$_2$(μ-P$_3$)]-[P$_3$C$_2$(COOMe)$_2$][b] (11)**	**[$^{\mathrm{Dipp}}$NHC-H]$_2$-[Cl][P$_7$(TMS)$_2$]**	
Formula	$C_{54}H_{72}AsN_4P_2$	$C_{60}H_{78}O_4N_4P_6$	$C_{72}H_{116}ClN_4O_3P_7Si_2$	
M	914.02	1105.08	1394.11	
Cryst. Syst.	Monoclinic	Monoclinic	Monoclinic	
Space Gr.	Cc	P2(1)/n	P2(1)/n	
A [Å]	10.2682(6)	23.6782(11)	22.3995(3)	
B [Å]	42.469(3)	18.3268(9)	12.1255(2)	
C [Å]	24.2300(12)	29.7342(14)	29.5997(5)	
α [deg]	90	90	90	
β [deg]	92.756	103.981(1)	90.820(1)	
Γ [deg]	90	90	90	
U [Å]	105540(11)	12520.8(10)	8038.6(2)	
Z	8	8	4	
total reflns.	23271	20284	24652	
Data Compl.	0.98	0.995	0.969	
Theta(max)	27.100	63.020	30.550	
R(reflns)	0.0456(16569)	0.0457(15958)	0.0456(17711)	
wR$_2$ (reflns)	0.1004(22831)	0.1073(20182)	0.1249(23887)	

a. All data collected at 100 K

b. Collected using a copper source at λ = 1.54178 Å.

EPR Studies

Continuous wave (CW) EPR spectra were recorded on a Bruker EMX 080 spectrometer equipped with a liquid nitrogen cooling system using a Bruker ER 4117 D-MVT resonator. The following experimental parameters were employed. For $(^{Dipp}NHC)_2(\mu\text{-}P_3)$ room temperature (frozen solution data is given in parenthesis) experiments were recorded at 9.33146 GHz (9.45748 GHz) using a modulation frequency of 100 kHz (100 kHz), a modulation amplitude of 1 G (2 G), and a microwave power of 0.02012 mW (0.02012 mW). For $(^{Dipp}NHC)_2(\mu\text{-PAsP})$ experiments at room temperature (frozen solution) were recorded at 9.476039 GHz (9.47366 GHz) using a modulation frequency of 100 kHz (100 kHz), a modulation amplitude of 0.5 G (2 G), and a microwave power of 0.6362 mW (0.02012 mW).

CW EPR spectra were computed with Matlab-8.1.0.604 using the EasySpin-4.5.0 package.[iv] Both frozen solution spectra were simulated with the function pepper, for the isotropic room temperature solution spectrum of $(^{Dipp}NHC)_2(\mu\text{-}P_3)$ garlic was employed, and chili for the room temperature solution spectrum of $(^{Dipp}NHC)_2(\mu\text{-PAsP})$ to include the rotational correlation time of the radical. Note the chili function only allows for one nucleus to be coupled to the electron spin.

Table S2: Spin Hamiltonian parameters for ($^{\mathrm{Dipp}}$NHC)$_2$(μ-P$_3$) and ($^{\mathrm{Dipp}}$NHC)$_2$(μ-PAsP). Hyperfine couplings and line widths (Gaussian, f.w.h.h.) are given in MHz. The DFT isotropic (A_{iso}) and anisotropic ($-T_1$, $-T_2$, T_1+T_2) hyperfine couplings are given in brackets under the experimental values.

($^{\mathrm{Dipp}}$NHC)$_2$(μ-P$_3$)				
Interaction	Principal values	Euler angles (radians)	A_{iso} ^{a}	$-T_1, -T_2, T_1+T_2$ ^{a}
g	2.0112, 2.0155, 2.0043	0, 0, 0	-	
Hyperfine central P atom (I = 1/2)	−9.3, −16.7, 505.0	3.1407, 0.2204, 1.5717	159.7 (137)	−169, −176, 345 (−169.2, −178.5, 347.7)
Hyperfine terminal P atoms (I = 1/2)	−21.1, −22.5, 74.0	∓0.6672, 0.2498, −π/2±0.1945	10.2 (17.8)	−31.2, −32.7, 63.9 (−27.7, −32.9, 60.6)
Linewidth	30, 20, 30	-		
($^{\mathrm{Dipp}}$NHC)$_2$(μ-PAsP)				
Interaction	Principal values	Euler angles (radians)	A_{iso} ^{a}	T_1, T_2, T_1+T_2 ^{a}
g	2.0695, 2.0326, 2.0017	0, 0, 0	-	
Hyperfine As (I = 3/2)	−120.7, −141.0, 435.7	0, 0.0913, 0	58.0 (45)	−178.7, −199.0, 377.7 (−153.4, −159.2, 312.6)
Hyperfine P atoms (I = 1/2)	−16.6, −6.3, 68.8	(±2.6322, 0.1222, π/2±0.0163)	15.3 (19.3)	−31.9, −21.6, 53.5 (−35.3, −28.0, 63.2)
Linewidth	50.6, 25.5, 48.3	-		

a. hyperfine coupling: $(A_1, A_2, A_3) = A_{\mathrm{iso}} + (-T_1, -T_2, T_1+T_2)$

Calculation of spin densities

The experimental spin densities for phosphorus and arsenic nuclei were estimated from their respective hyperfine couplings, $\rho^{total} = \rho_s + \rho_p = A_{iso} / S_0^{DFT} + T / P_0^{DFT}$, where S_0^{DFT} and P_0^{DFT} are coupling constants for s-type and p-type spin density (d-type orbital contributions were negligibly small). Values for S_0^{DFT} and P_0^{DFT} in each case were computed from the DFT data, e.g. $S_0^{DFT} = A_{iso}^{DFT} / \rho_s^{DFT}$ where A_{iso}^{DFT} is the Fermi contact hyperfine coupling and ρ_s^{DFT} is the Mulliken atomic spin density for s-type orbitals as given by the DFT results. Similarly, $P_0^{DFT} = T^{DFT} / \rho_p^{DFT}$, where $T = (T_1+T_2)/2$.

For $(^{Dipp}NHC)_2(\mu\text{-}P_3)$ the experimental (DFT) Mulliken spin densities are: 64.4% (65.6%) is located on the central phosphorus, and 3.8% (3.3%) on each of the other two (terminal) P atoms. For $(^{Dipp}NHC)_2(\mu\text{-}PAsP)$ the experimental (DFT) Mulliken spin densities are: 80.4% (67.3%) is located on the central arsenic, and 1.5% (2.0%) on each of the other two (terminal) P atoms.

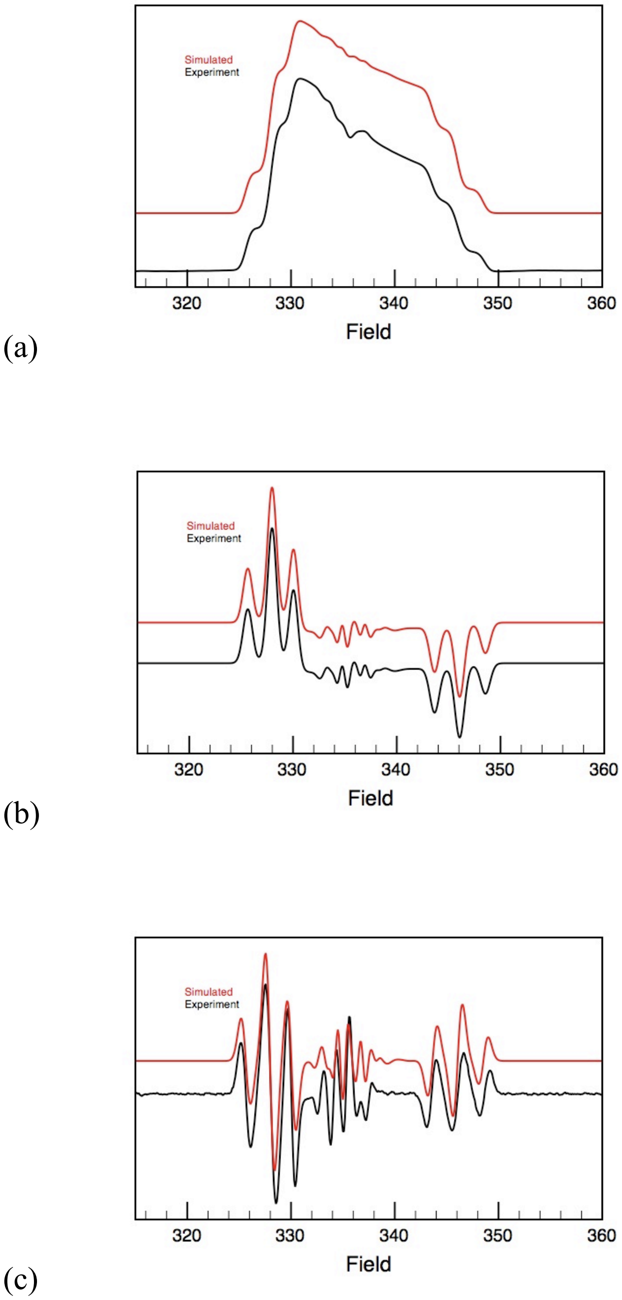

Figure S1. Experimental (black) and simulated (red) X-band (9.457481 GHz) CW EPR spectra of $(^{\mathrm{Dipp}}\mathrm{NHC})_2(\mu\text{-}P_3)$ obtained at 80 K in n-hexane. The absorption spectrum (a) and the 2nd harmonic (c) is computed from the measured 1st harmonic spectrum (b) by integration and differentiation, respectively.

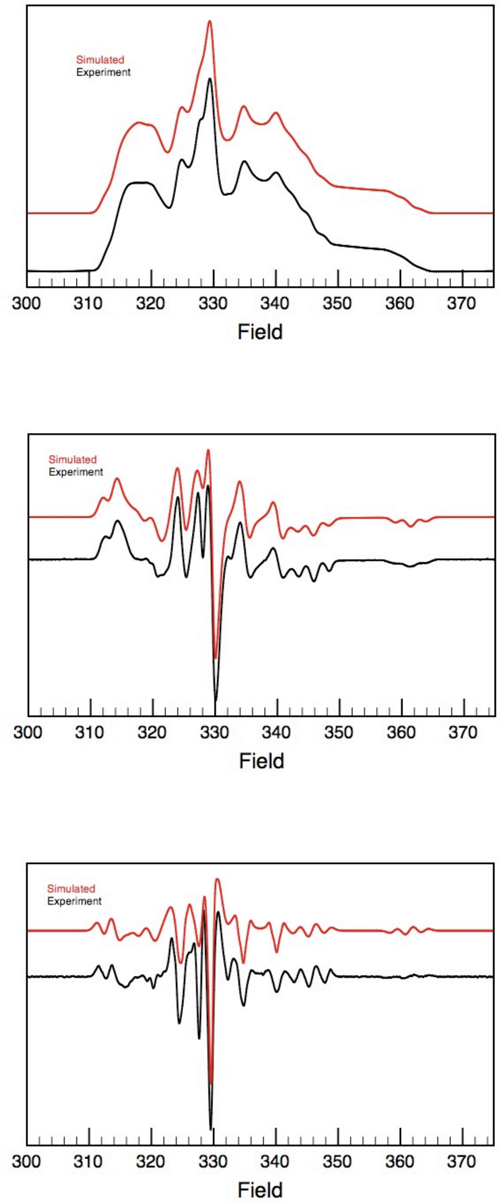

(a)

(b)

(c)

Figure S2. Experimental (black) and simulated (red) X-band (9.47366 GHz) CW EPR spectra of $(^{\mathrm{Dipp}}\mathrm{NHC})_2(\mu\text{-PAsP})$ obtained at 80 K in n-hexane. The absorption spectrum (a) and the 2nd harmonic (b) is computed from the measured 1st harmonic spectrum (c) by integration and differentiation, respectively.

Synthesis of ^{Dipp}NHC=PH (4).

A 100 mL round bottom flask was charged with 0.250 g (0.573 mmol) of [^{Dipp}NHC-H][Cl] and 0.210 g (0.600 mmol) Na(OCP). Under argon flow, 50 mL of THF was added and, while open to a mineral oil bubbler, the reaction was refluxed for 4 hours. The volatiles were removed and the residue was triturated with 25 mL of toluene and filtered over a glass frit three times. The combined toluene washes were evaporated under reduced pressure. The off-white residue was washed with diethyl ether and volatiles were removed under reduced pressure. The ether from the wash was placed at −35 °C overnight and the precipitate was filtered and volatiles were removed under reduced pressure. The products were combined to yield 0.180 g (71% based on imidazolium salt). Single crystals suitable for X-ray diffraction were grown from a slowly evaporating THF solution of ^{Dipp}NHC=PH. Analysis for **$C_{27}H_{37}N_2P_1$**: Calculated C = 77.11%, H = 8.87%, N = 6.66%. Experiment C = 76.17%, H = 8.82%, N = 6.31%. **MP**: 215-218 °C. **^{1}H NMR** (C_6D_6) δ (ppm) = 7.27-7.08 (m, 6H, *Ar*), 6.18 (s, 2H, C*H*=C*H*), 3.04 (sep, $^3J_{HH}$ = 6.7 Hz, 4H, *CH*(CH$_3$)$_2$), 1.92 (d, $^1J_{PH}$ =165 Hz, 1H, P-*H*), 1.45 (d, $^3J_{HH}$ = 6.7 Hz, 12H, CH(C*H*$_3$)$_2$) 1.14 (d, $^3J_{HH}$ = 6.7 Hz, 12H, CH(C*H*$_3$)$_2$). **^{13}C NMR** (C_6D_6) δ (ppm) = 180.18 (d, $^1J_{PC}$ = 86 Hz, *C*=P), 147.86, 135.09, 130.58, 125.02, 119.59, 29.37 (s, *C*H(CH$_3$)$_2$), 24.88 (s, CH(*C*H$_3$)$_2$), 24.23 (s, CH(*C*H$_3$)$_2$). **^{31}P{^{1}H} NMR** (C_6D_6) δ (ppm) = 136.68 (s). **^{31}P NMR** (C_6D_6) δ (ppm) = 136.68 (d, $^1J_{PH}$ = 164 Hz). **UV/Vis** (23 °C, THF, [nm]) = 319, 211.

Alternative Synthesis (a) of ^{Dipp}NHC=PH (4).

A 100 mL round bottom Schlenk flask was charged with 1.00 g (2.292 mmol) of $P_7(TMS)_3$ and 1.0 g (2.353 mmol) of [^{Dipp}NHC-H][Cl]. 50 mL of THF was added to the mixed solids and the yellow solution was stirred for 48 hours, after which time the color had changed to dark red. The solvent was removed under reduced pressure, and the residue was triturated with n-hexane and filtered at room temperature. The solution was cooled to −78 °C and the light yellow crystals were isolated and volatiles were removed under reduced pressure on a glass frit. The remaining red solid was triturated with toluene, and the yellow solution was filtered and the toluene was removed under reduced pressure, yielding an off-white powder. The combined yield of ^{Dipp}NHC=PH was 0.692 g (70% based on imidazolium salt).

Alternative Synthesis (b) of ^{Dipp}NHC=PH (4).

The synthesis of ^{Dipp}NHC=PH was carried out according to the above procedure with the exception of the following: the yellow THF solution containing 1.00 g (2.292 mmol) of $P_7(TMS_3)$ and 2.0 g (4.705 mmol) of [^{Dipp}NHC-H][Cl] was refluxed for 4 hours, cooled to room temperature, and allowed to stir overnight. The yield was 0.705 g of ^{Dipp}NHC=PH (36% based on imidazolium salt).

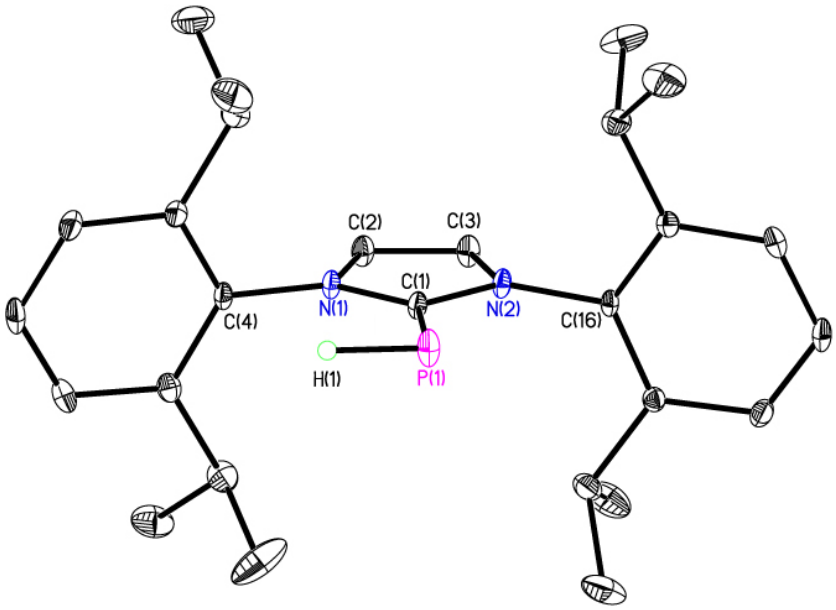

Figure S3. Solid-state structure of ^{Dipp}NHC=PH. Hydrogen atoms (except for P-*H*) are omitted for clarity. Ellipsoids are shown at 30% probability.

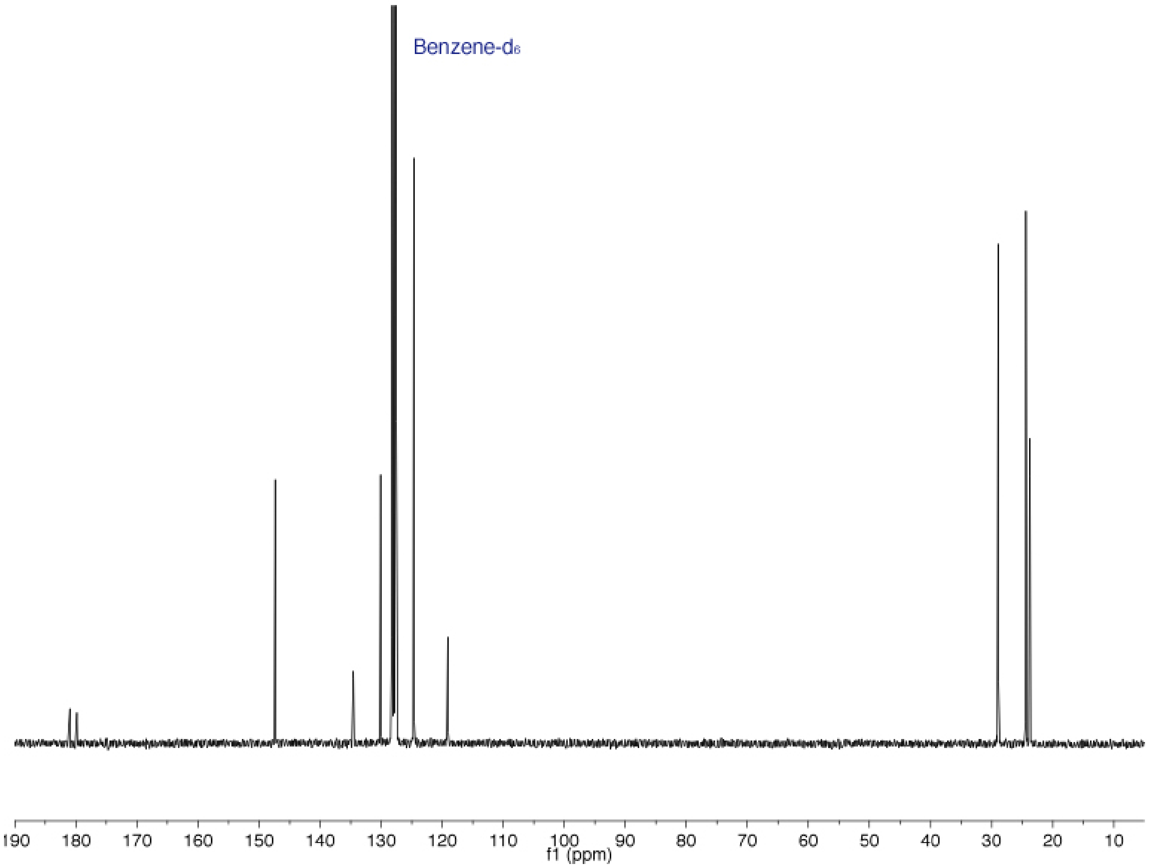

Figure S4. ^{13}C spectrum of ^{Dipp}NHC=PH (**4**) acquired at 298K and 125.790 MHz in C_6D_6.

Synthesis of [(^{Dipp}NHC)$_2$(μ-P$_3$)][Cl] (7).

In a 50mL Schlenk flask, 0.200 g (0.471 mmol) of ^{Dipp}NHC=PH (**4**) and 0.060 g (0.475 mmol) DABCO were dissolved in 25 mL of THF. Under a flow of argon, 0.032 g freshly distilled PCl_3 (0.235 mmol) was added dropwise via microsyringe. There was an immediate color change from yellow to green upon addition, as well as formation of a colorless precipitate. The solution was stirred for one hour, at which time the green solution was filtered over Celite. The solution was reduced to a third of the initial volume, and 15 mL n-hexane was added inducing the precipitation of the green [(^{Dipp}NHC)$_2$(μ-P$_3$)][Cl]. The compound was collected on a glass frit, rinsed with n-hexane and volatiles were removed under reduced pressure to yield 0.135 g (64%) of [(^{Dipp}NHC)$_2$(μ-P$_3$)][Cl]. X-ray quality single crystals were grown from a slowly evaporating

THF solution of $[(^{\mathrm{Dipp}}\mathrm{NHC})_2(\mu\text{-}\mathrm{P}_3)][\mathrm{Cl}]$. Analysis for $\mathbf{C_{54}H_{72}ClN_4P_3}$: Calculated C = 71.62%, H = 8.01%, N = 6.19%. Experiment C = 70.59%, H = 8.38%, N = 6.18%. **MP**: > 220 °C. **MS** (MALDI) Calculated m/z = 869.4970, Experiment m/z = 869.4965. ^{1}**H NMR** ($\mathrm{C}D_2\mathrm{Cl}_2$) δ (ppm) = 7.48 (t, $^{3}J_{\mathrm{HH}}$ = 7.8 Hz, 4H, p-*Ar*), 7.32 (s, 2H, NHC C*H*=C*H*), 7.22 (d, $^{3}J_{\mathrm{HH}}$ = 7.8 Hz, 8H, m-*Ar*), 2.39 (sep, $^{3}J_{\mathrm{HH}}$ = 6.7 Hz, 8H, *CH*($\mathrm{CH_3}$)$_2$), 1.13 (d, $^{3}J_{\mathrm{HH}}$ = 6.7 Hz, 8H, *CH*($\mathrm{CH_3}$)$_2$) 1.05 (d, $^{3}J_{\mathrm{HH}}$ = 6.7 Hz, 8H, *CH*($\mathrm{CH_3}$)$_2$). ^{13}**C NMR** ($\mathrm{C}D_2\mathrm{Cl}_2$) δ (ppm) = 161.37 (t, 48 Hz, *C*=P), 145.80 (s, Ar*C*-^{i}Pr), 132.03 (s, Ar*C*-NHC), 131.98 (s, Ar *p*-*C*), 125.58 (s, NHC *C*H=*C*H), 125.49 (s, Ar *m*-*C*), 29.67 (s, *C*H($\mathrm{CH_3}$)$_2$), 24.27 (s, CH($C\mathrm{H_3}$)$_2$), 23.42 (s, CH($C\mathrm{H_3}$)$_2$). ^{31}**P NMR** ($\mathrm{C}D_2\mathrm{Cl}_2$) δ (ppm) = 591.88 (t, $^{1}J_{\mathrm{PP}}$ =505.9 Hz), 190.59 (d, $^{1}J_{\mathrm{PP}}$ =505.9 Hz). **UV/Vis** (23 °C, THF, [nm]) = 666, 434, 331, 269, 219.

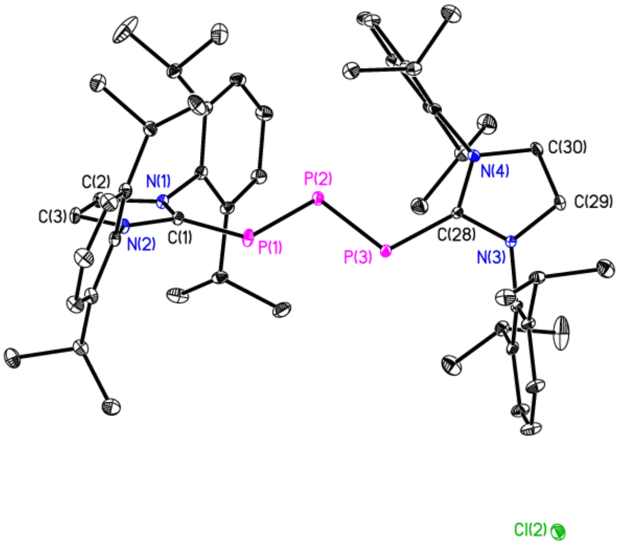

Figure S5. Solid-state structure of $[(^{\mathrm{Dipp}}\mathrm{NHC})_2(\mu\text{-}\mathrm{P}_3)][\mathrm{Cl}]$ (**7**). Hydrogen atoms and THF molecules are omitted for clarity. Ellipsoids are shown at 30% probability.

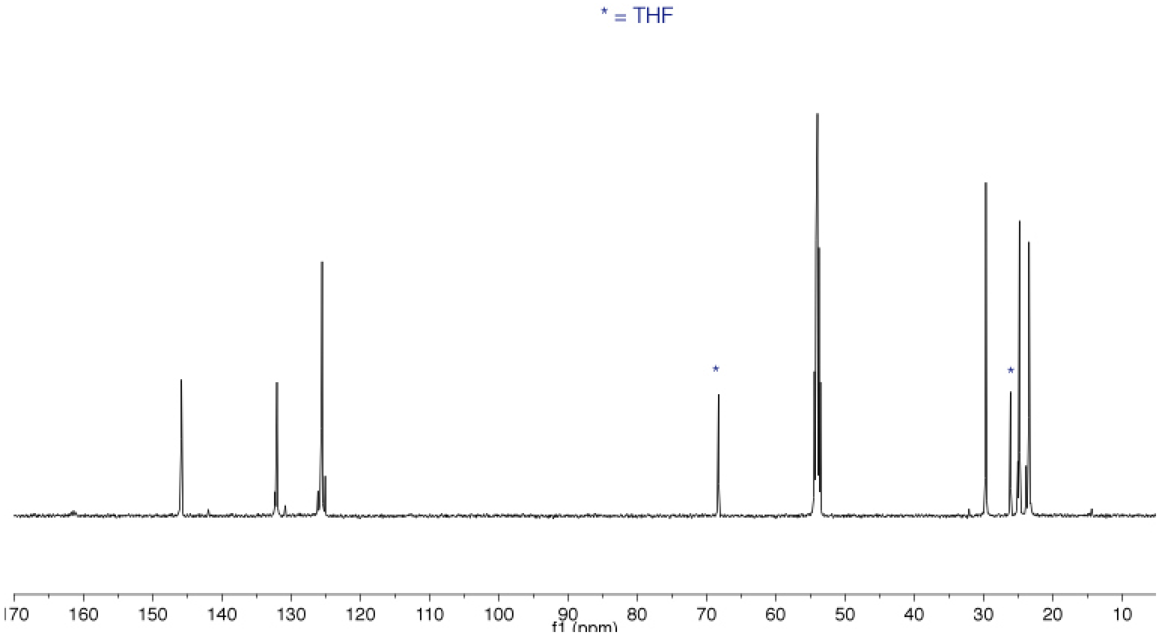

Figure S6. 125.790 MHz ^{13}C spectrum of [(^{Dipp}NHC)$_2$(μ-P$_3$)][Cl] acquired at 298K in C*D*$_2$Cl$_2$.

Synthesis of (^{Dipp}NHC)$_2$(μ-P$_3$) (9).

A 15 mL scintillation vial was charged with 0.100 g (0.110 mmol) of [(^{Dipp}NHC)$_2$(μ-P$_3$)][Cl] (**7**) and 7 mL of THF. To the stirring solution an excess of Mg^0 (0.050 g, 2.056 mmol) was added. Stirring was continued until the color changed from green to dark purple. THF was removed under reduced pressure and n-hexane were added to the residue to extract (^{Dipp}NHC)$_2$(μ-P$_3$) (**9**). The solution was then filtered over Celite. The volume of n-hexane was reduced to roughly 1/3 of the initial volume and the vial was cooled to −35 °C upon which 0.054 g (56%) of a dark powder of (^{Dipp}NHC)$_2$(μ-P$_3$) (**9**) were formed. Single crystals suitable for X-ray diffraction were grown from a concentrated n-hexane solution at −35 °C. Analysis for **$C_{54}H_{72}N_4P_3$**: Calculated C = 74.54%, H = 8.34%, N = 6.44%. Experiment C = 72.91%, H = 8.25%, N = 6.10%. **MP**: 115 °C (decomposition). **UV/Vis** (23 °C, n-hexane, [nm]) = 776, 638, 516, 340, 300, 225.

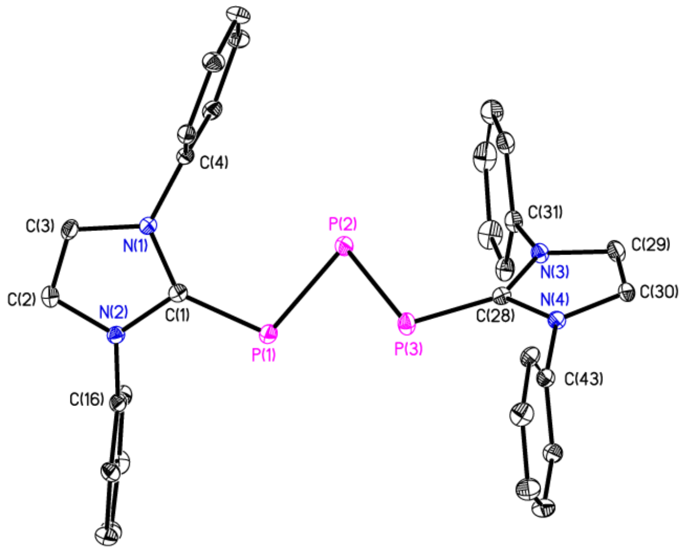

Figure S7. Solid-state structure of (^{Dipp}NHC)$_2$(μ-P$_3$) (**9**). Hydrogen atoms and *iso*-propyl groups are omitted for clarity. Ellipsoids are shown at 30% probability.

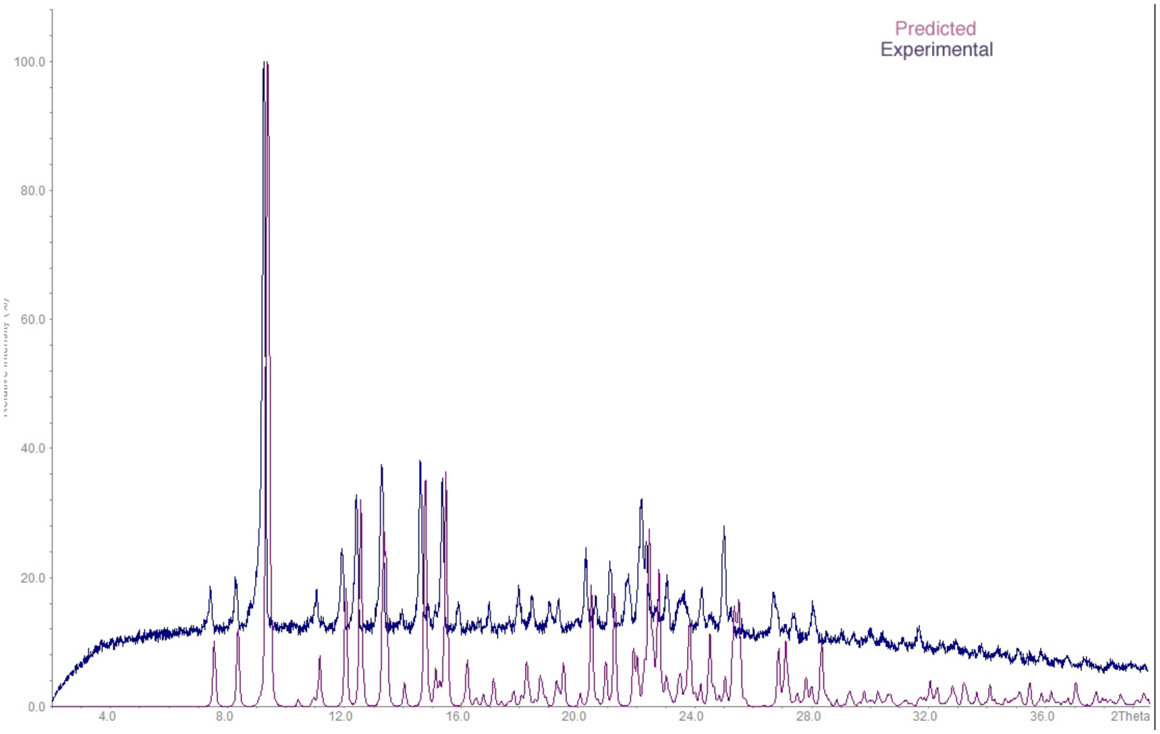

Figure S8. Experimental and simulated powder X-ray diffraction pattern of (^{Dipp}NHC)$_2$(μ-P$_3$) (**9**).

Synthesis of [(^{Dipp}NHC)$_2$(μ-PAsP)][Cl] (8).

In a 50 mL Schlenk flask, 0.300 g (0.706 mmol) of ^{Dipp}NHC=PH (**4**) and 0.090 g (0.707 mmol) DABCO were dissolved in 25 mL of THF. Under a flow of argon, 0.064 g (0.353 mmol) of $AsCl_3$ was added drop-wise via microsyringe. There was an immediate color change from yellow to green upon addition, as well as formation of a colorless precipitate. The solution was stirred for one hour, at which time the green solution was filtered over Celite. The solution was reduced to a third of the initial volume, and 15 mL of n-hexane was added inducing the precipitation of the green [(^{Dipp}NHC)$_2$(μ-PAsP)][Cl] (**8**). The compound was collected on a glass frit, rinsed with n-hexane and volatiles were removed under reduced pressure to yield 0.185 g (55%) of [(^{Dipp}NHC)$_2$(μ-PAsP)][Cl] (**8**). X-ray quality single crystals were grown from a slowly evaporating THF solution of [(^{Dipp}NHC)$_2$(μ-PAsP)][Cl] (**8**). Analysis for **$C_{54}H_{72}ClN_4P_2As$**: Calculated C = 68.31%, H = 7.64%, N = 5.90%. Experiment C = 64.52%, H = 7.32%, N = 5.31%. **MS** (MALDI) Calculated m/z = 913.4448, Experiment m/z = 913.4444. **MP**: 185 °C (decomposition). **^{1}H NMR** (CD_2Cl_2) δ (ppm) = 7.49 (t, $^3J_{HH}$ = 7.8 Hz, 4H, p-*Ar*), 7.40 (s, 2H, NHC C*H*=C*H*), 7.23 (d, $^3J_{HH}$ = 7.8 Hz, 8H, m-*Ar*), 2.41 (sep, $^3J_{HH}$ = 6.9 Hz, 8H, *CH*(CH_3)$_2$), 1.14 (d, $^3J_{HH}$ = 6.9 Hz, 24H, CH(C*H*$_3$)$_2$) 1.05 (d, $^3J_{HH}$ = 6.9 Hz, 24H, CH(C*H*$_3$)$_2$). **^{13}C NMR** (CD_2Cl_2) δ (ppm) = 162.96 (t, 44.0 Hz, *C*=P), 145.42 (s, Ar*C*-^{i}Pr), 132.18 (s, Ar*C*-NHC), 132.05 (s, Ar *p*-*C*), 125.66 (s, Ar *m*-*C*), 125.41 (s, NHC *C*H=*C*H), 29.08 (s, *C*H(CH_3)$_2$), 24.32 (s, CH(*C*H$_3$)$_2$), 22.88 (s, CH(*C*H$_3$)$_2$). **^{31}P NMR** (CD_2Cl_2) δ (ppm) = 218.92 (s). **UV/Vis** (23 °C, THF, [nm]) = 714, 454, 339, 242.

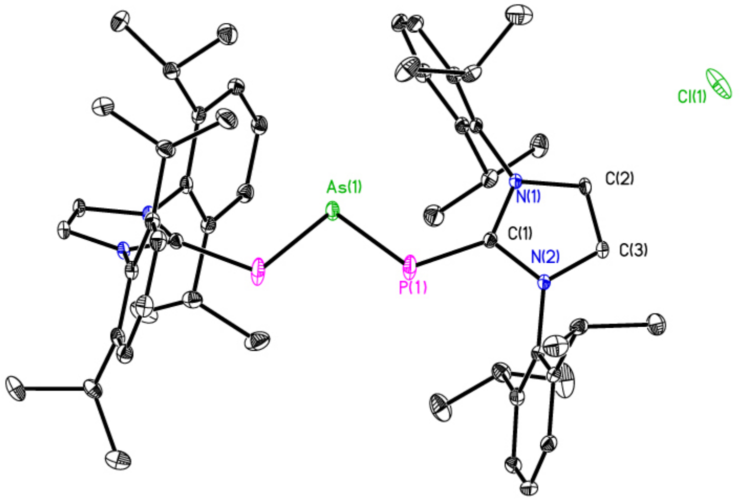

Figure S9. Solid-state structure of [(^{Dipp}NHC)$_2$(μ-PAsP)][Cl]. Hydrogen atoms and THF are omitted for clarity. Ellipsoids are shown at 30% probability.

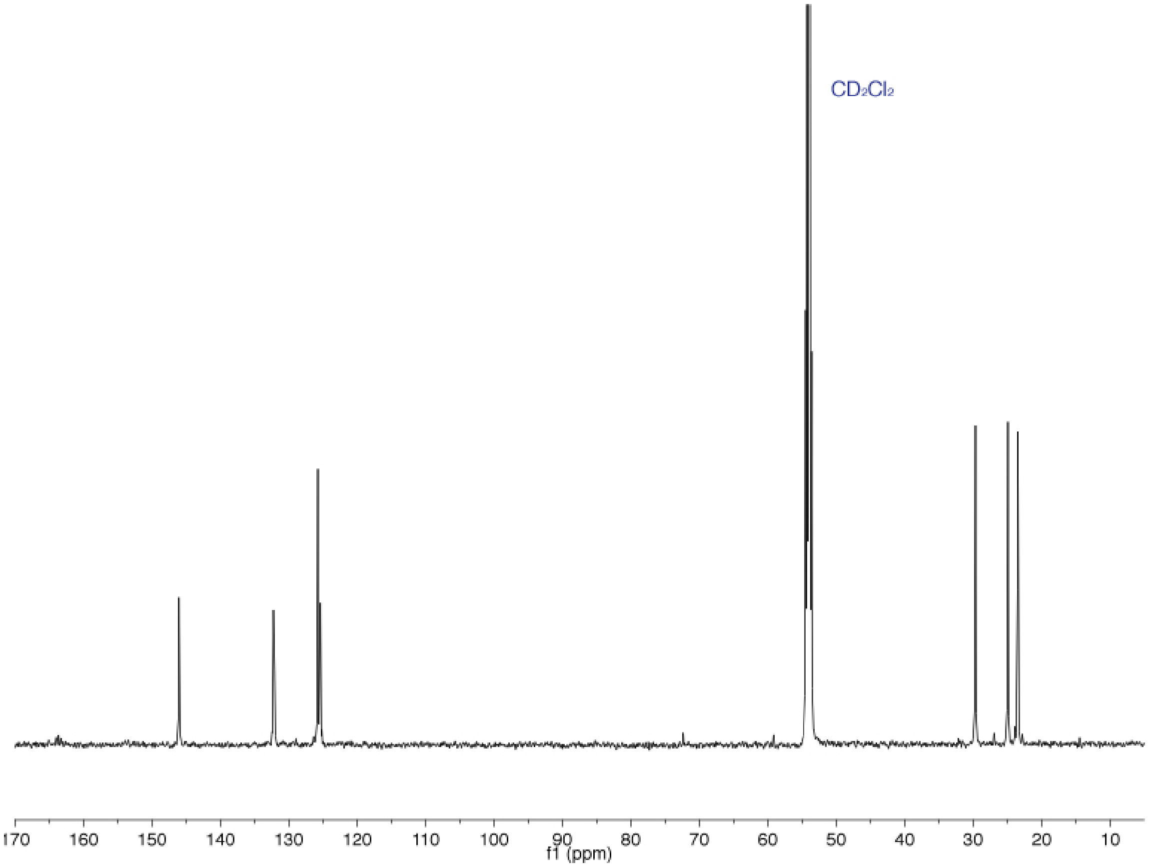

Figure S10. The 125.790 MHz ^{13}C spectrum of [(^{Dipp}NHC)$_2$(μ-PAsP)][Cl] acquired at 298K in CD_2Cl$_2$.

Synthesis of (^{Dipp}NHC)$_2$(μ-PAsP) (10).

A 15 mL scintillation vial was charged with 0.100 g (0.105 mmol) of [(^{Dipp}NHC)$_2$(μ-PAsP)][Cl] (**8**) and 7 mL of THF. An excess of Mg^0 (0.050 g, 2.056 mmol) was added to the stirring solution. Stirring was continued until the color changed from green to dark purple. THF was removed under reduced pressure and n-hexane were added to the residue, extracting (^{Dipp}NHC)$_2$(μ-PAsP) (**10**). The volume of n-hexane was reduced by 1/3 and the vial was cooled to −35 °C and 0.035 g (36%) of a dark powder of (^{Dipp}NHC)$_2$(μ-PAsP) were formed (**10**). Single crystals suitable for X-ray diffraction were grown in the same fashion. Analysis for **$C_{54}H_{72}N_4P_2As$**: Calculated C = 70.96%, H = 7.94%, N = 6.13%. Experiment C = 69.81%, H = 7.89%, N = 6.31%. **MP**: 92 °C (decomposition). **UV/Vis** (23 °C, n-hexane, [nm]) = 772, 605, 524, 353, 306, 228.

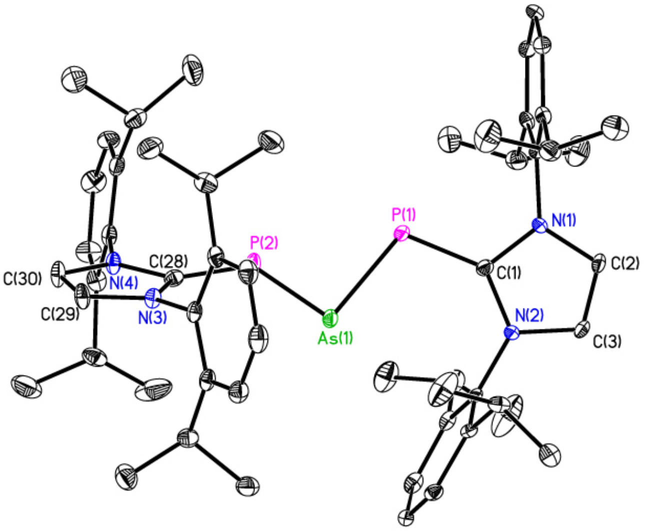

Figure S11. Solid-state structure of (^{Dipp}NHC)$_2$(μ-PAsP). Hydrogen atoms are omitted for clarity. Ellipsoids are shown at 30% probability.

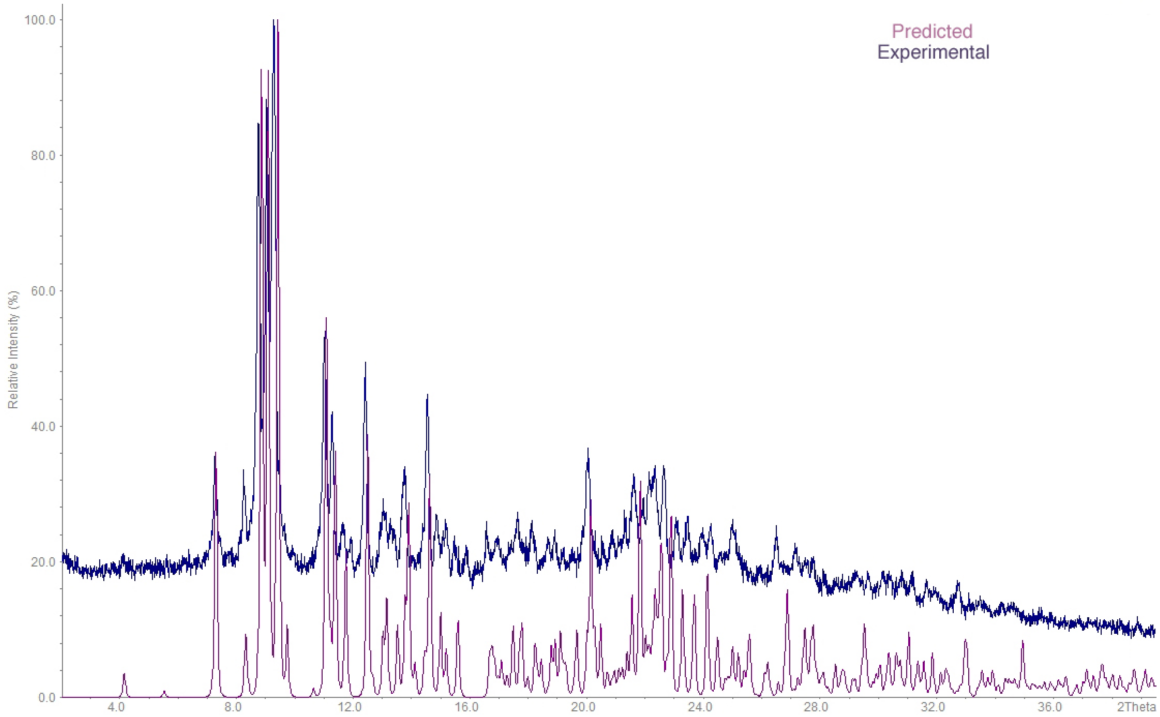

Figure S12. Experimental and simulated powder X-ray diffraction pattern of $(^{Dipp}NHC)_2(\mu\text{-PAsP})$.

Synthesis of $[(^{Dipp}NHC)_2(\mu\text{-}P_3)]$[4,5-di(methylcarboxy)-1,2,3-triphospholide] (11).

A 15 mL scintillation vial was charged with 0.050 g (0.055 mmol) of $[(^{Dipp}NHC)_2(\mu\text{-}P_3)][Cl]$ (**7**) and 2 mL of THF. An excess of Mg^0 (0.025 mg, 1.028 mmol) was added to the stirring solution. The reaction was stirred until a dark blue color replaced the green color, typically 1 to 2 hours. The THF was removed until the residue was a sticky solid, and 5 mL of n-hexane was used to extract the radical by filtering the solution through Celite. A 0.10 M solution of dimethylacetylene dicarboxylate (0.006 g (0.046 mmol), 83% of the calculated amount based on $[(^{Dipp}NHC)_2(\mu\text{-}P_3)][Cl]$) in THF was added dropwise until the blue color of the solution was replaced by a green precipitate. The green precipitate was collected on a glass frit and volatiles were removed under reduced pressure to give 0.020 g (65%) of a green powder identified as $[(^{Dipp}NHC)_2(\mu\text{-}P_3)]$[4,5-di(methylcarboxy)-1,2,3-triphospholide] (**11**). Crystals suitable for X-ray diffraction were grown from a slowly evaporating THF solution. Analysis for **$C_{60}H_{78}N_4O_4P_6$**: Calculated C = 65.21%, H = 7.11%, N = 5.07%. Experiment C = 65.57%, H = 7.61%, N = 5.65%. **MS** (MALDI) Calculated m/z = 869.4970, Experiment m/z = 869.4965. **MP** =134-137. **^{1}H NMR** (THF-*d*$_8$) δ (ppm) = 7.45 (t, $^{3}J_{HH}$ = 8.0 Hz, 2H, p-*Ar*), 7.30 (s, 2H, NHC C*H*=C*H*), 7.25 (d, $^{3}J_{HH}$ = 8.0 Hz, 4H, m-*Ar*), 3.46 (s, 3H, COOC*H$_3$*), 3.44 (s, 3H, COOC*H$_3$*) 2.45 (sep, $^{3}J_{HH}$ = 6.9 Hz, 8H, *CH*(CH$_3$)$_2$), 1.13 (d, $^{3}J_{HH}$ = 6.9 Hz, 24H, CH(C*H$_3$*)$_2$) 1.08 (d, $^{3}J_{HH}$ = 6.9 Hz, 24H, CH(C*H$_3$*)$_2$). **^{13}C NMR** (THF-*d*$_8$) δ (ppm) = 146.46 (s, Ar*C*-^{i}Pr), 133.11, 132.76, 129.20, 126.98, 125.89, 51.22 (s, COO*C*H$_3$), 50.28 (s, COO*C*H$_3$), 30.20 (s, CH(*C*H$_3$)$_2$), 24.80 (s, CH(*C*H$_3$)$_2$), 23.75 (s, CH(*C*H$_3$)$_2$). **^{31}P NMR** (THF-*d*$_8$) δ (ppm) = 591.75 (t, $^{1}J_{PP}$ = 505.6 Hz), 306.41-291.40 (m, AA'B simulated as: δ $P_{A,A'}$= 302.31, δ P_B= 294.76, $J_{PAPA'}$ = 91.60 Hz, J_{PAPB} = 475.76 Hz), 190.16 (d, $^{1}J_{PP}$ = 505.6 Hz). **UV/Vis** (23 °C, THF, [nm]) = 669, 428, 331, 276, 208.

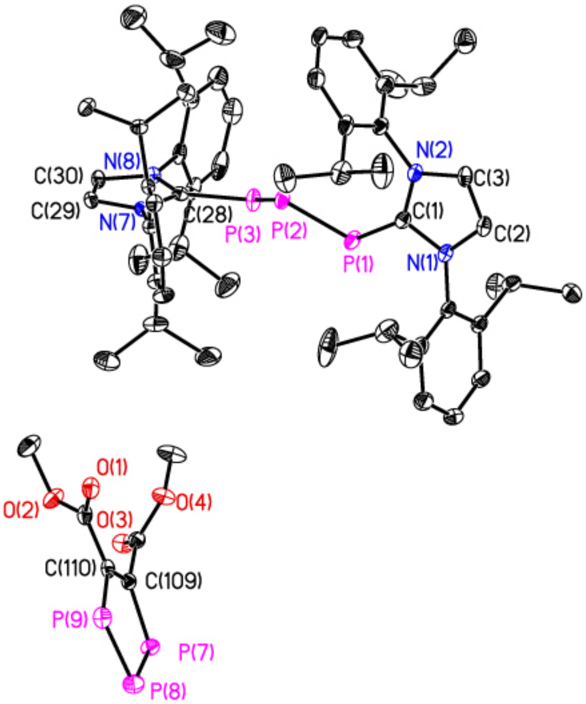

Figure S13. Solid-state structure of [(^{Dipp}NHC)$_2$(μ-P$_3$)][4,5-di(methylcarboxy)-1,2,3-triphospholide]. One of the two molecules of the asymmetric unit cell is shown. Hydrogen atoms are omitted for clarity. Ellipsoids are shown at 30% probability.

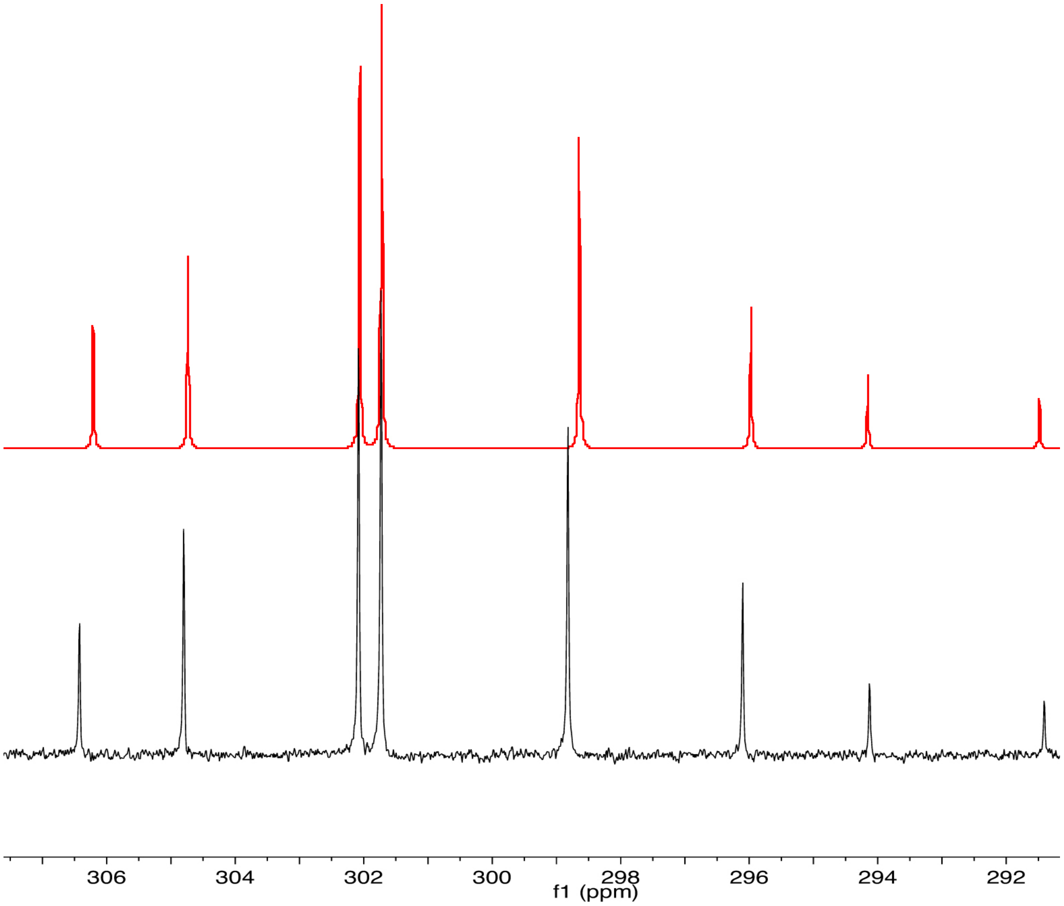

Figure S14. Region of the AA'B system of the 1,2,3-phospholide and the simulated spectrum (shown in red).

Observation of [^{Dipp}NHC-H]$_2$[P$_7$TMS$_2$][Cl]

A 15 mL scintillation vial was charged with 0.200 g (0.458 mmol) of P$_7$(TMS)$_3$ and it was dissolved in 4 mL of THF. To the stirring solution 2 equivalents of ^{Dipp}NHC-HCl was added with stirring. When the solid had dissolved completely, the solution was filtered through Celite into another vial, which was placed at −35 °C and layered with n-hexane. Pale yellow single crystals suitable for X-ray diffraction grew overnight. ^{31}**P NMR** (THF) δ = -192 – -

202.54 (m), -169.55 – -180.77 (m), -103.35 – -112.95 (m), -78.27 – -88.90 (m), -55.69 – -75.85 (m), -38.16 – -29.00 (m), -15.88 – -28.63 (m).

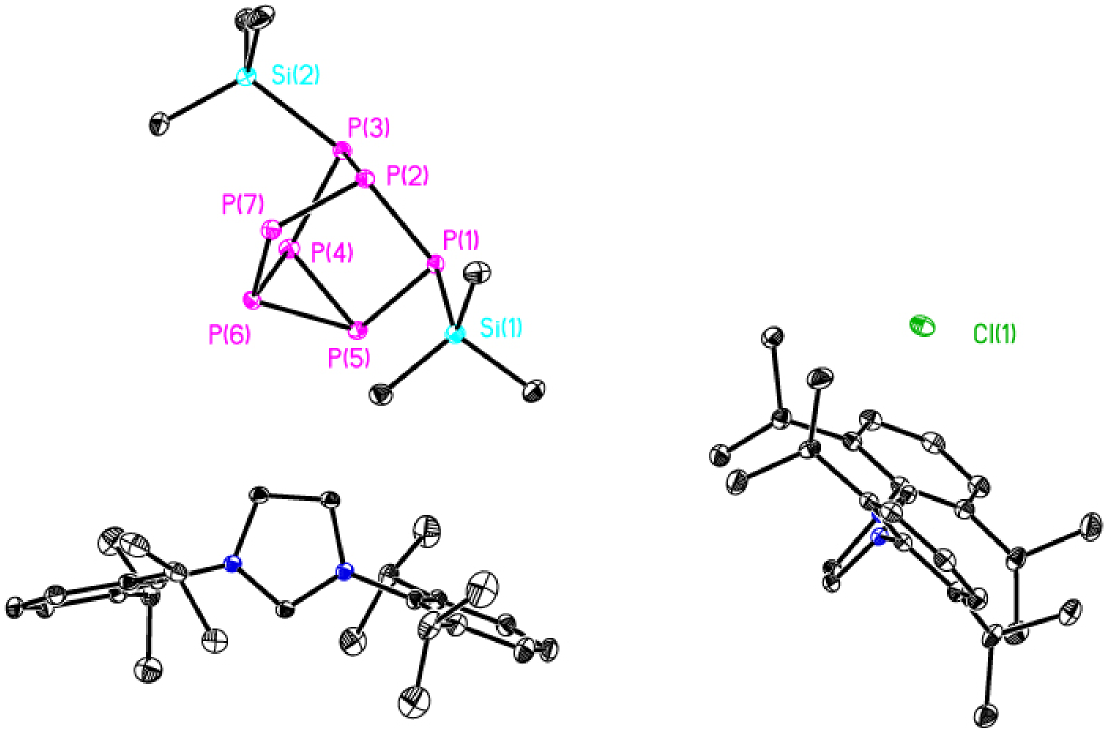

Figure S15. Solid-state structure of [$^{\text{Dipp}}$NHC-H]$_2$[P$_7$TMS$_2$][Cl]. Hydrogen atoms and THF solvent molecules are omitted for clarity. Ellipsoids are shown at 30% probability.

Computations

The computations were carried out with the Gaussian 09 program package. All structures were optimized with the 6-31+G* basis set using the B3LYP functional. The AIM and NBO analysis was performed at the B3LYP/cc-pVDZ//B3LYP/6-31+G* level of theory. At the optimized structures vibrational analysis was performed to check whether the stationary point located is a minimum of the potential energy hypersurface or a first order saddle point (for transition states). At the saddle points IRC calculations were performed to locate the minima connected by the transition structure. The NBO analysis was performed with the NBO 5.0 program. For visualization of the molecules the Molden program was used.

Notes:

[Note1] The viability of route (ii) is supported by the observations that imidazolium-based ionic liquids may generate free carbenes. Although the N-heterocyclic carbenes (imidazol-2-ylidenes) are remarkably strong Brønsted bases, the deprotonation of their conjugated acids (imidazolium cations) is possible with superbases (e.g. alkoxide ions). A comprehensive computational study on the possible isomeric structures of imidazolium salts revealed that the basicity of the counter anion is an important factor in the formation of carbene–acid adducts. If the basicity of the anion is small (e.g. OTf^- or NTf_2^-), only a hydrogen-bonded ion pair could be optimized in the gas phase. However, the more basic anions (e.g. CH_3COO^-) can compete for the proton with the carbene: the relative energy of the adduct of the carbene and the protonated anion (Brønsted acid) is rather similar to that of the corresponding anion–cation pair, and in the vapor of the ‘salt’ this former adduct was indeed observed experimentally.

[Note2] The bonding situation in phosphinidene-carbene adducts was studied in detail by Frison and Sevin, who analysed the contribution of the three limiting resonance structures **A**–**C**.

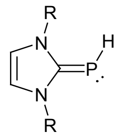

A

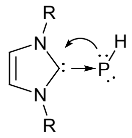

B

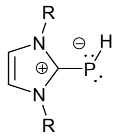

C

While **A** represents an ideal C=P double bond, **C** is an ylidic description. Nevertheless, ELF investigations, the analysis of bond lengths and rotational barriers as well as nucleus independent chemical shift (NICS) calculations suggest the dominancy of resonance structure **B**. Thus, the CP bonding essentially is derived from the σ-donation from the carbene to the PH moiety, but a substantial π-backbonding was also found decreasing slightly the aromaticity of the five-membered ring compared to the free carbene.

For **7A** the most likely resonance structures shown below have been taken into consideration. Since the bonding between a PR unit and the imidazole moiety was established using the σ-donation π-back bonding model (structure **B**), here we only show the mesomeric structures with such CP bonds.

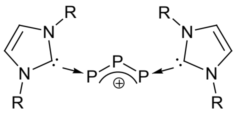

D

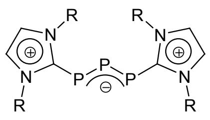

E

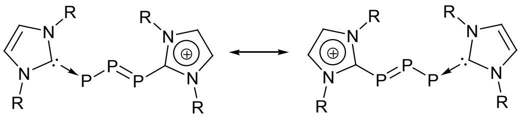

F **F'**

The mesomeric structure **D** localizes the positive charge on the P_3 moiety. This structure can be excluded according to the NPA and Mulliken charges, since the three phosphorus atoms are almost neutral. The significant contribution of structure **E** can likewise be neglected, as it proposes negatively charged P atoms.

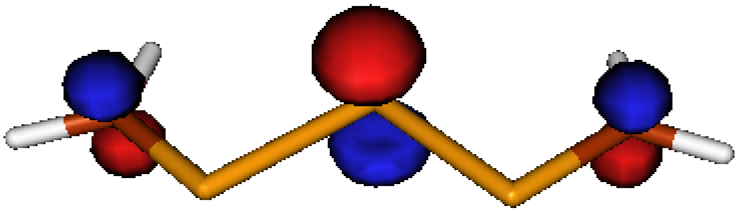

Figure S16. SOMO of $(H_2C)_2(\mu\text{-}P_3)$ at the B3LPY/6-31G* level.

Table S3. NPA and Mulliken charges (in electrons) at the B3LYP/cc-pVDZ//B3LYP/6-31+G* level of theory.

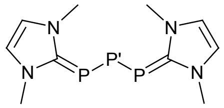	Cation		Radical	
	NPA	Mulliken	NPA	Mulliken
P’ (central)	−0.06	−0.07	−0.26	−0.26
P	+0.07	−0.05	−0.04	−0.18
Imidazol ring	+0.45	+0.59	+0.17	+0.31
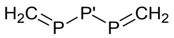	Cation		Radical	
	NPA	Mulliken	NPA	Mulliken
P’ (central)	+0.25	+0.16	−0.06	−0.07
P	+0.42	+0.22	+0.33	+0.07
CH_2 unit	−0.04	+0.19	−0.30	−0.04

Table S4. Geometrical parameters of $[(^{Me}NHC)_2(\mu\text{-}P_3)]^+$ isomers at the B3LYP/6-31+G* level of theory

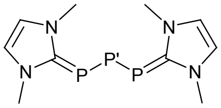	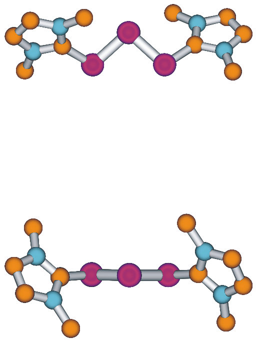	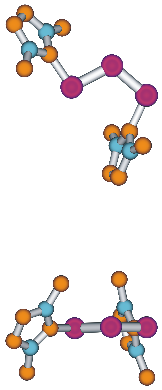	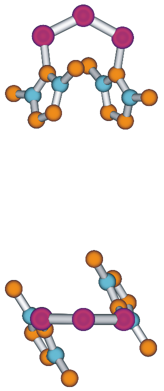
E (kcal/mol)	**0.0**	**1.4**	**12.9**
CP	1.840	1.841 1.850	1.839
PP’	2.115	2.122 2.104	2.118
CPP’	97.1	96.7 105.3	110.6
PP’P	102.7	111.7	124.1
CPP’P	177.1	179.0 0.6	17.3
CPPC	−8.3	179.2	32.4
NCPP’	−63.3	62.2 79.9	59.0

NCPP’: to describe torsion of the imidazole ring out of the plane of the three phosphorus atoms, the smallest NCPP’ torsional angle is shown.

Table S5. Geometrical parameters of $(^{Me}NHC)_2(\mu\text{-}P_3)$ isomers at the B3LYP/6-31+G* level of theory

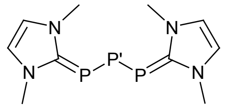	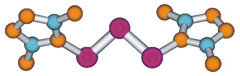	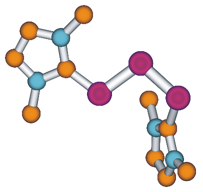	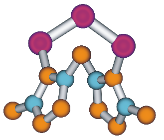	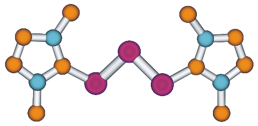
	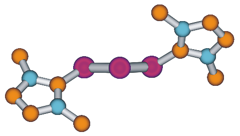	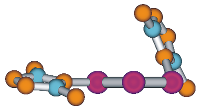	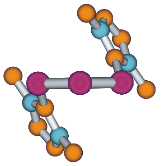	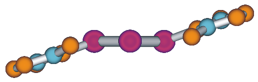
E (kcal/mol)	**0.0**	**1.4**	**3.8**	**0.9**
CP	1.795	1.793 1.805	1.801	1.789
PP’	2.187	2.196 2.187	2.202	2.192
CPP’	103.1	106.5 107.0	108.5	105.7
PP’P	95.8	101.2	111.5	92.1
CPP’P	152.6	−179.6 42.3	38.6	160.7
CPPC	−84.8	−138.0	73.7	−68.5
NCPP’	−36.0	−15.4 44.7	41.0	19.4

NCPP’: to describe torsion of the imidazole ring out of the plane of the three phosphorus atoms, the smallest NCPP’ torsional angle is shown.

Cartesian coordinates and total energies

I

HF = −760.069863

N	−0.032597	−0.042989	0.155653
C	−0.045722	−0.141763	1.542938
C	1.255993	−0.142365	1.933991
N	2.009554	−0.043810	0.769099
C	1.234694	0.018958	−0.357197
C	3.464736	−0.009863	0.740481
C	−1.231281	−0.005981	−0.669865
P	2.075926	1.140535	−3.295340
C	2.556969	1.330168	−4.923470
O	2.873059	1.596262	−6.013068
H	1.696589	−0.201106	2.918944
H	−0.956206	−0.199754	2.122049
H	−1.870327	0.836481	−0.383175
H	−0.918910	0.117657	−1.707387
H	−1.799584	−0.937604	−0.569834
H	3.882296	−0.946257	1.127487
H	3.775401	0.123479	−0.296351
H	3.842070	0.825836	1.340037
H	2.189041	−0.267631	−3.458772

TS1

HF = −760.070807

C	0.105494	0.165228	−0.000404
C	0.105559	0.165235	1.359691
N	1.426400	−0.020541	1.750214
C	2.255178	−0.140680	0.679543
N	1.426298	−0.020553	−0.391050
C	1.881429	−0.080659	3.135827
C	1.881196	−0.080683	−1.776705
P	5.546812	0.032230	0.679305
C	5.444353	1.693218	0.679246
O	5.396714	2.868353	0.679201
H	−0.703772	0.281302	2.065758
H	−0.703903	0.281288	−0.706395
H	1.430599	−0.936819	−2.289158
H	1.613095	0.840411	−2.303632
H	2.966162	−0.190579	−1.773761
H	1.430903	−0.936806	3.648322
H	2.966397	−0.190524	3.132781
H	1.613351	0.840429	3.662778
H	3.976056	−0.042177	0.679445

II

HF = −760.072004

C	0.120430	0.420457	−0.405708
N	−0.273200	−0.086548	0.827943
C	0.786546	−0.322531	1.657348
N	1.855388	0.056081	0.895186
C	1.475990	0.511289	−0.362887
C	−1.658088	−0.337288	1.204249
P	0.769022	−1.674681	5.085746
C	0.645617	−0.126629	5.727215
O	0.559732	0.918343	6.242828
C	3.234944	−0.009334	1.358798
H	−0.578847	0.668340	−1.191235
H	2.183949	0.853539	−1.103929
H	3.825773	−0.672018	0.717125
H	3.688115	0.987950	1.360165
H	3.229732	−0.403157	2.375657
H	−2.113682	−1.070432	0.529776
H	−1.664290	−0.730818	2.221221
H	−2.239468	0.590575	1.172578
H	0.772543	−1.097210	3.746982

III

HF = −760.069863

N	−0.032597	−0.042989	0.155653
C	−0.045722	−0.141763	1.542938
C	1.255993	−0.142365	1.933991
N	2.009554	−0.043810	0.769099
C	1.234694	0.018958	−0.357197
C	3.464736	−0.009863	0.740481
C	−1.231281	−0.005981	−0.669865
P	2.075926	1.140535	−3.295340
C	2.556969	1.330168	−4.923470
O	2.873059	1.596262	−6.013068
H	1.696589	−0.201106	2.918944
H	−0.956206	−0.199754	2.122049
H	−1.870327	0.836481	−0.383175
H	−0.918910	0.117657	−1.707387
H	−1.799584	−0.937604	−0.569834
H	3.882296	−0.946257	1.127487
H	3.775401	0.123479	−0.296351
H	3.842070	0.825836	1.340037
H	2.189041	−0.267631	−3.458772

TS2

HF = −760.062953

C	0.020070	−0.049509	−0.001634
C	0.021544	−0.051425	1.358387
N	1.350791	0.030149	1.750449
C	2.186151	0.075064	0.676094
N	1.348542	0.032476	−0.396458
C	1.803219	0.047675	3.138524
C	1.796606	0.053229	−1.786084
P	4.312340	0.821731	0.666180
C	6.101897	1.474704	0.679347
O	6.863631	2.351200	0.655799
H	−0.793375	−0.098808	2.065715
H	−0.796361	−0.094606	−0.707354
H	1.261168	0.831598	−2.338209
H	2.865276	0.274100	−1.791574
H	1.617026	−0.918074	−2.258681
H	1.667330	−0.937214	3.597498
H	2.861585	0.314028	3.144212
H	1.237000	0.794081	3.703677
H	4.783669	−0.504661	0.762529

4A

HF = −646.783013

C	−0.143197	0.000000	0.007980
N	0.013172	0.000000	1.379584
C	1.361516	0.000000	1.714014
C	2.064443	0.000000	0.555734
N	1.144679	0.000000	−0.490401
C	1.482518	0.000000	−1.899821
H	3.128648	0.000000	0.377170
H	1.693752	0.000000	2.740706
C	−1.101435	0.000000	2.306636
P	−1.722633	0.000000	−0.790783
H	−1.171280	0.000000	−2.105008
H	−0.713315	0.000000	3.327447
H	−1.723635	0.889250	2.150907
H	−1.723635	−0.889250	2.150907
H	2.570432	0.000000	−1.997234
H	1.076349	−0.890192	−2.393016
H	1.076349	0.890192	−2.393016

CO

HF = −113.317323

C	−0.020920	0.000000	1.322922
O	0.964021	0.000000	1.891578

$[(^{Me}NHC)_2(\mu\text{-}P_3)]^+$

HF = −1633.569575

N	−0.240745	−0.217951	0.021238
C	−0.157449	−0.227119	1.381596
N	1.111378	0.171407	1.678270
C	1.809476	0.435340	0.516240
C	0.960633	0.200044	−0.520780
P	−1.338993	−0.849237	2.646776
P	−2.922574	0.481636	2.204736
P	−4.448858	−0.160869	3.520787
C	−5.685753	1.128496	3.083266
N	−5.641865	2.482902	3.229027
C	−6.871146	3.030290	2.911153
C	−7.697033	2.000283	2.582053
N	−6.957746	0.838747	2.689788
C	−4.497208	3.268713	3.697974
C	−7.483831	−0.507648	2.442445
C	1.673217	0.279664	3.028580
C	−1.396161	−0.630386	−0.780360
H	−8.734107	1.995231	2.283308
H	−7.051156	4.093837	2.948532
H	1.107291	0.290664	−1.586243
H	2.837165	0.764821	0.526031
H	−4.875967	4.183715	4.157005
H	−3.946246	2.688675	4.439993
H	−3.835064	3.518678	2.866031
H	−8.405592	−0.414745	1.866118
H	−6.751951	−1.086239	1.876641
H	−7.692240	−1.014509	3.388392
H	−1.034024	−0.968954	−1.752792
H	−1.906564	−1.451452	−0.274459
H	−2.089686	0.202910	−0.913345
H	2.574578	0.892250	2.976485
H	0.944398	0.751552	3.689411
H	1.924916	−0.710923	3.416580

$[(H_2C)_2(\mu\text{-}P_3)]^+$

HF = −1102.316165

P	0.323091	−0.314141	0.279058
P	0.385673	0.350227	2.350522
P	2.380307	0.004905	−0.354651
C	2.085800	−0.568007	−1.949179
H	2.912214	−0.582758	−2.661666
H	1.133992	−0.929455	−2.338601
C	−1.279244	0.012755	2.616394
H	−1.703658	0.213536	3.601471

H	−1.979403	−0.392828	1.885984

$(^{Me}NHC)_2(\mu\text{-}P_3)$

HF = −1633.723774

C	0.127034	0.125410	−0.059204
N	0.389794	0.763465	1.138094
C	1.668444	0.448173	1.577688
C	2.224416	−0.383654	0.661934
N	1.280207	−0.589591	−0.330384
C	1.467956	−1.429641	−1.500837
H	3.194854	−0.855053	0.634312
H	2.064058	0.841570	2.501565
C	−0.436882	1.796128	1.751078
P	−1.239651	0.167152	−1.221591
P	−2.985491	0.387083	0.076163
P	−4.233855	1.405067	−1.402420
C	−5.899536	0.967452	−0.897429
N	−6.965114	1.822782	−1.115505
C	−8.155044	1.223025	−0.737397
C	−7.848780	−0.008924	−0.259732
N	−6.473314	−0.168976	−0.359861
C	−5.795930	−1.440830	−0.138371
H	−8.482406	−0.783733	0.144014
H	−9.104241	1.728397	−0.828803
C	−6.843223	3.158953	−1.672884
H	0.183407	2.348237	2.462310
H	−0.801421	2.475947	0.976029
H	−1.299588	1.365876	2.263591
H	2.339916	−2.067920	−1.336569
H	0.574254	−2.043390	−1.651411
H	1.623605	−0.822914	−2.399837
H	−6.558118	−2.220540	−0.057401
H	−5.139926	−1.654594	−0.986716
H	−5.187953	−1.417543	0.768201
H	−7.776654	3.698722	−1.493834
H	−6.009213	3.676908	−1.188929
H	−6.644863	3.119575	−2.749757

$(H_2C)_2(\mu\text{-}P_3)$

HF = −1102.610281

P	0.160569	−0.370939	0.166644
P	0.305693	0.253276	2.252068
P	2.253576	−0.091081	−0.384688
C	2.183977	−0.569550	−2.013344
H	3.097806	−0.548444	−2.605493
H	1.290765	−0.904644	−2.539140

C	−1.314886	0.048021	2.722795
H	−1.596402	0.281334	3.748679
H	−2.122325	−0.303740	2.081810

---

[i] D. Heift, Z. Benkő and H. Grützmacher, *Dalt. Trans.* 2014, **43**, 831-840.

[ii] H. Schmidbauer and A. Bauer, *Phosphorus, Sulfur, and Silicon and the Related Elements*, 1995, **102**, 217-219.

[iii] P. Tang, W. Wang and T. Ritter, *J. Am. Chem. Soc.*, 2011, **133**, 11482-11484.

[iv] S.Stoll, and A. Schweiger, EasySpin, a comprehensive software package for spectral simulation and analysis in EPR. *J. Magn. Res.*, 2006, **178**, 42.